Accepted Manuscript

Development of novel liver X receptor modulators based on a 1,2,4-triazole scaffold

Shaimaa S. Goher, Kristine Griffett, Lamees Hegazy, Mohamed Elagawany, Mohamed M.H. Arief, Amer Avdagic, Subhashis Banerjee, Thomas P. Burris, Bahaa Elgendy

PII: S0960-894X(18)30970-3
DOI: https://doi.org/10.1016/j.bmcl.2018.12.025
Reference: BMCL 26194

To appear in: *Bioorganic & Medicinal Chemistry Letters*

Received Date: 26 September 2018
Revised Date: 30 November 2018
Accepted Date: 12 December 2018

Please cite this article as: Goher, S.S., Griffett, K., Hegazy, L., Elagawany, M., Arief, M.M.H., Avdagic, A., Banerjee, S., Burris, T.P., Elgendy, B., Development of novel liver X receptor modulators based on a 1,2,4-triazole scaffold, *Bioorganic & Medicinal Chemistry Letters* (2018), doi: https://doi.org/10.1016/j.bmcl.2018.12.025

Graphical Abstract

To create your abstract, type over the instructions in the template box below.
Fonts or abstract dimensions should not be changed or altered.

Development of novel liver X receptor modulators based on a 1,2,4-triazole scaffold

Leave this area blank for abstract info.

Shaimaa S. Goher, Kristine Griffett, Lamees Hegazy, Mohamed Elagawany, Mohamed M. H. Arief, Amer Avdagic, Subhashis Banerjee, Thomas P. Burris, and Bahaa Elgendy

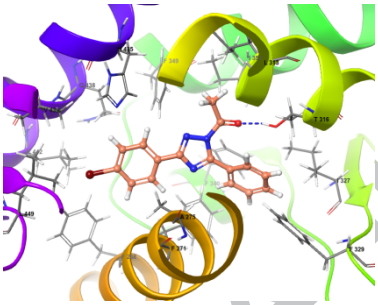

8b

EC_{50} = 113 nM (LXRα), 231 nM (LXRβ)

Bioorganic & Medicinal Chemistry Letters
journal homepage: www.elsevier.com

Development of novel liver X receptor modulators based on a 1,2,4-triazole scaffold

Shaimaa S. Goher[a], Kristine Griffett[b], Lamees Hegazy[c], Mohamed Elagawany[c], Mohamed M. H. Arief[a], Amer Avdagic[b], Subhashis Banerjee[c], Thomas P. Burris[b], and Bahaa Elgendy[a,b,*]

[a]*Chemistry Department, Faculty of Science, Benha University, Benha 13518, Egypt*
[b]*Center for Clinical Pharmacology, Washington University School of Medicine and St. Louis College of Pharmacy, St. Louis, MO 63110, USA*
[c]*Department of Pharmacology and Physiology, Saint Louis University School of Medicine, St. Louis, MO 63104, USA*

ARTICLE INFO

Article history:
Received
Revised
Accepted
Available online

Keywords:
Liver X receptor
Agonist
1,2,4-Triazole
HCV
ADME

ABSTRACT

Liver X Receptor (LXR) agonists have been reported as a potential treatment for atherosclerosis, Alzheimer's disease and hepatitis C virus (HCV) infection. We have designed and synthesized a series of potent 1,2,4-triazole scaffolds as novel LXR modulators. In cell-based cotransfection assays these compounds generally functioned as LXR agonists and we observed compounds with selectivity towards LXRα (7-fold) and LXRβ (7-fold) in terms of potency. Assessment of the effects of selected compounds on LXR target gene expression in HepG2 cells revealed that compounds **6a-b** and **8a-b** behaved as inverse agonists on FASN expression even though they were agonists in the LXRα and LXRβ cotransfection assays. Interestingly, these compounds had no effect on the expression of SREBP-1c confirming a unique LXR modulator pharmacology. Molecular docking studies and evaluation of ADME properties *in-silico* show that active compounds possess favorable binding modes and ADME profiles. Thus, these compounds may be useful for in vivo characterization of LXR modulators with unique profiles and determination of their potential clinical utility.

* Corresponding author. Tel.: +1-314-446-8336; fax: +1-314-446-8136; e-mail: belgendy@wustl.edu

Liver X receptors (LXRs) have emerged as a promising drug targets because they effectively regulate lipid metabolism and inflammation. LXRs are known as oxysterol receptors and have two isoforms, LXRα (NR1H3) and LXRβ (NR1H2). In humans, LXRα consists of 447 amino acids and is expressed mainly in liver, kidney, intestine, adipose tissue, and macrophages; LXRβ consists of 460 amino acids and is expressed ubiquitously.[1,2]

A growing body of literature indicates that LXR is a potential drug target for a range of diseases. LXR agonists have been shown to increase reverse cholesterol transport and reduce atherosclerosis by targeting induction of ATP-binding Cassette Transporter A1 (ABCA1) gene expression.[2-7] Agonists have also been shown to have anti-inflammatory activity.[2,8,9] Efficacy in Alzheimer's disease models and cancer models has also been demonstrated for LXR agonists.[2,8,,10-14] Stimulation of hepatic lipogenesis by agonists (via stimulation of transcription of SREBP-1c, FASN, and SCD1) has limited development of agonists for treatment of these diseases.

This has led to efforts to develop LXR modulators that would display tissue selective gene modulation effects (e.g. ABCA1) so as to retain the ability to activate key beneficial pathways while avoiding those that are detrimental (e.g. SREBP-1c). The potential utility of LXR ligands has continued to expand. LXR agonists have been shown to reduce the replication of hepatitis C virus via targeting key genes that are required for HCV replication.[15] Based on the ability of LXR to regulate de novo lipogenesis, we have evaluated LXR inverse agonists for their ability to suppress tumor growth and to treat non-alcoholic steatohepatitis with success .[14,16]

Compound **3** is a new LXR modulator that was recently identified using pharmacophore modeling and shape-based virtual screening.[17] When this compound was evaluated in an LXR luciferase reporter gene assay, it showed moderate partial agonist activity compared to LXR full agonist GW3965 (**2**). Development of a partial agonist may be advantageous since LXR full agonists have been demonstrated to cause severe adverse side effects due to elevation of hepatic lipogenesis. There is no additional structure-activity-relationship (SAR) data in the literature on compound **3**. The 1,2,4-triazole heterocycle is an important building block for the synthesis of biologically active molecules and found wide variety of applications in medicinal chemistry.[18,19]

As part of our ongoing research to discover novel LXR modulators of clinical importance,[14,16] we developed new LXR agonists based on the 1,2,4-triazole scaffold **3** to evaluate them as potential drugs.

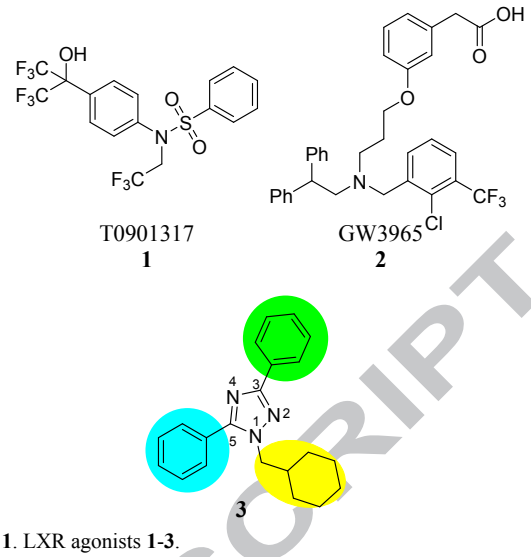

Figure 1. LXR agonists **1-3**.

We have synthesized a library of new LXR agonists based on 1,2,4-triazole scaffold **3**, which we divided into three parts as highlighted in Figure 1. We studied the structure activity relationships (SAR) by modifying these three parts, namely substituents at N-1, C-3, and C-5 through different chemical transformations. The structures of synthesized compounds were elucidated using different spectroscopic techniques.

3,5-disubstituted-1*H*-1,2,4-triazoles (**6a-l**) were synthesized by reacting nitriles (**4a,b**) with hydrazides (**5a-l**) in *n*-butanol in the presence of anhydrous potassium carbonate at 150 °C.[20] The synthesized triazoles (**6a,d,e,g**) reacted with different alkyl halides in DMF to give 1-alkyl-3,5-disubstituted-1*H*-1,2,4-triazoles (**7a-l**).[21] Acetyl triazoles (**8a-e**) were obtained by refluxing 3,5-disubstituted-1*H*-1,2,4-triazoles (**6a,e,f,g,i**) with acetic anhydride. Sulphonyl derivatives (**9a,b**) were obtained via reacting **6a,g** with *p*-toluene sulfonyl chloride in presence of suitable base (Scheme 1).

We evaluated the activity of synthesized compounds in a cell based (HEK293 cells) cotransfection assay using either full-length human LXRα or LXRβ and a reporter containing 3 copies of an LXR response element (LXRE) within the promoter of a luciferase reporter gene. We initially decided to evaluate the activity of 3,5-disubstituted-1*H*-1,2,4-triazoles (**6a-l**) as the core scaffold of ligand **3**. Testing these compounds against both LXR isoforms showed potent agonistic activity. The parent triazole **6a** showed potent agonist activity against LXRα (EC_{50} for LXRα = 142 nM) and moderate activity against LXRβ (EC_{50} for LXRβ = 1008 nM). Compound **6a** was 7-fold selective for LXRα over LXRβ. Then, we explored the effect of substituents on the phenyl ring at C-3 (R^2). Electron withdrawing substituents at 2-position of the phenyl ring (**6b** and **6c**) showed good agonistic activity against both LXR isoforms, higher efficacy toward LXRβ, and slight selectivity toward LXRα (Table 1). Switching the position of Cl and Br from 2-position to 4-position (**6d** and **6e**) enhanced the agonistic activity against both LXR isoforms and reversed the selectivity toward LXRβ (Table 1).

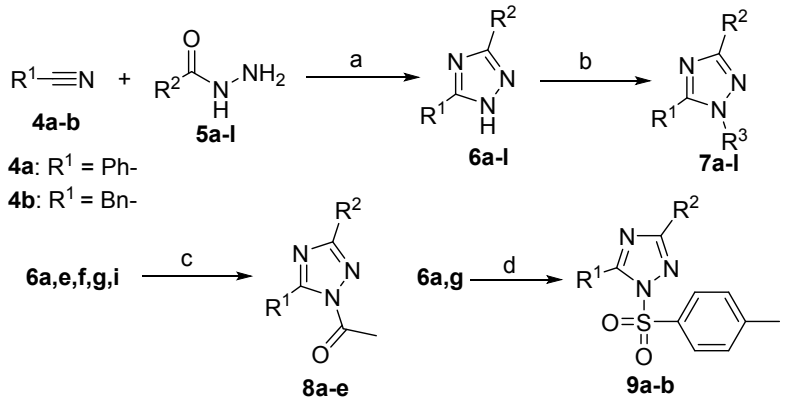

Scheme 1. Reagents and conditions: (a) K_2CO_3, *n*-BuOH, 150 °C; (b) R^3Cl, K_2CO_3, DMF, reflux; (c) Ac_2O, reflux 2-3 h; (d) TsCl, pyridine, reflux 6 h

Table 1. LXR activity of 1,2,4-triazole derivatives **6a-l**

			LXRα		LXRβ			
Compound	**R^1**	**R^2**	**EC_{50} (nM)**	**E_{max} (%)**	**EC_{50} (nM)**	**E_{max} (%)**	**EC_{50} α/β**	**ClogP**
6a	Ph-	Ph-	142	56	1008	63	0.14	3.40
6b	Ph-	2-Cl-Ph-	526	60	640	74	0.82	3.57
6c	Ph-	2-Br-Ph-	390	52	493	67	0.79	3.63
6d	Ph-	4-Cl-Ph-	309	51	245	60	1.26	3.64
6e	Ph-	4-Br-Ph-	164	55	68	62	2.41	3.73
6f	Ph-	4-CH_3-Ph-	77	62	85	73	0.91	3.50
6g	Ph-	3-CH_3O-Ph-	108	60	68	72	1.59	3.24
6h	Ph-	3-Pyridyl	ia	-	ia	-	-	2.32
6i	Ph-	$PhCH_2$-	2202	45	6152	59	0.36	3.54
6j	$PhCH_2$-	Ph-	ia	-	ia	-	-	3.52
6k	$PhCH_2$-	2-Cl-Ph-	570	46	966	61	0.59	3.87
6l	$PhCH_2$-	4-Cl-Ph-	ia	-	2573	73	-	3.99

ia = inactive at 10 μM

[a] E_{max} (%) is the percentage ratio between maximum fold induction of the tested compound and fold induction for **1** at 10 μM.

Electron donating groups on the phenyl ring of R^2 enhanced the agonistic activity against both LXR isoforms significantly. Compound **6f** with CH_3 group at 4-position was potent dual agonist for LXRα (EC_{50} for LXRα = 77 nM) and LXRβ (EC_{50} for LXRβ = 85 nM). Similarly, compound **6g** was potent dual agonist (EC_{50} = 108 and 68 nM, for LXRα and LXRβ, respectively), but more selective toward LXRβ by 1.6-fold. Compound **6g** was docked in the LBP of LXRβ (Figure 2A). The ligand makes mainly hydrophobic contacts with Ile309, Met312, Leu313, Ile327, Phe329 and Leu274. The tautomer of compound **6g** makes hydrogen bonding interaction through the hydrogen atom on N-1 to Thr271. Methoxy group made another hydrogen bond with Thr316, which is likely responsible for higher potency of compound **6g** over compound **6a** that lacks hydrogen-bond donor at this position.

When we replaced the phenyl group in **6a** with 3-pyridyl group in **6h**, the compound lost the agonistic activity against both isoforms. Interestingly, the clogP of this compound is the lowest in this series and this might be the reason for the loss of activity. Replacing the phenyl group in **6a** with benzyl group in **6i** reduced the agonistic activity for both LXR isoforms but showed ≈ 2.8-fold selectivity toward LXRα (Table 1).

Changing substituents at C-5 (R^1) from phenyl group (**6a**) to benzyl group (**6j**), diminished the agonistic activity toward both LXRα and LXRβ. Substituting the phenyl group at C-3 of **6j** with chlorine in 2-position (**6k**) regained the agonistic activity toward LXRα (EC_{50} = 570 nM) and LXRβ (EC_{50} = 966 nM). Transposition of chlorine atom to 4-position (**6l**) rendered the compound inactive against LXRα and lowered the activity toward LXRβ by ≈ 4.9-fold compared to **6j** and by ≈ 2.7-fold compared to **6k**. Addition of CH_2 as a linker between the triazole ring and the phenyl ring at C-5 in **6j**, **6k**, and **6l** caused the geometry to be tilted in all three compounds if compared to their corresponding derivatives, **6a**, **6b**, and **6d**. This change in the geometry might affect the complementarity of **6j**, **6k**, and **6l** within the binding site and disrupt their π-π stacking with the surrounding aromatic residues. For example, compound **6b** was predicted to make π-π stacking with Phe271, Phe340, Phe329 and a halogen bond with Thr316 but the change in geometry in **6k** due to the extra CH_2, led to flipping of the binding pose and loss of the halogen bond interaction and one of the π-π stacking interactions (Figure S1). Similarly, if we compare **6d** to **6l**, the addition of CH_2 linker led to less complementarity of the ligand within the binding pocket where CH_2 group was displaced out of the hydrophobic region and located instead in a hydrophilic region (Figure S2). Therefore, we suggest that aromatic substitution at C-5 (R^1) is important to maintain good agonistic activity.

Next, we investigated the effect of substituting N-1 with different alkyl groups while maintaining R^1 as a phenyl group and changing the substituent pattern at R^2 by synthesizing compounds **7a-l** (Table 2). Alkylating compound **6a** with different alkyl groups provided compounds **7a-e**. Substituting N-1 with methyl group in **7a** reduced the agonistic activity dramatically toward LXRα (≈7-fold) and slightly toward LXRβ (≈ 2.6-fold) if compared to the parent triazole **6a**. Compounds **7b-e** with an ethyl, butyl, ally, and benzyl groups at N-1 were very weak agonists against LXRα and completely inactive against LXRβ (Table 2). Compound **7f** where R^2 is 3-methoxy phenyl and R^3 is benzyl group showed moderate agonistic activity against LXRα (EC_{50} for LXRα = 903 nM), and weak activity against LXRβ (EC_{50} for LXRβ = 2365 nM). This compound was ≈ 2.6-fold more selective toward LXRα over LXRβ. On the contrary, the corresponding analogue, **6g**, was more selective toward LXRβ over LXRα by ≈ 1.6-fold. Comparison of the docking poses of compounds **6g** and **7f** in the LBP of LXRβ predicts that adding alkyl groups at the N-1 position disrupted the ligand's complementarity in the ligand binding pocket leading to flipped binding pose for compound **7f** and loss of both hydrogen bonds formed by compound **6g** tautomer with amino acid residues Thr316 and Phe271 (Figure 2B).

Table 2. LXR activity of 1,2,4-triazole derivatives **7a-l**

				LXRα		LXRβ			
Comp.	**R¹**	**R²**	**R³**	**EC_{50} (nM)**	**E_{max} (%)**	**EC_{50} (nM)**	**E_{max} (%)**	**EC_{50} α/β**	**ClogP**
7a	Ph-	Ph-	CH_3-	2468	64	2637	71	0.94	3.69
7b	Ph-	Ph-	C_2H_5-	ia	-	ia	-	-	4.92
7c	Ph-	Ph-	C_4H_9-	2470	65	ia	-	-	5.08
7d	Ph-	Ph-	C_3H_5-	ia	-	ia	-	-	4.56
7e	Ph-	Ph-	$PhCH_2$-	2178	58	ia	-	-	5.40
7f	Ph-	3-CH_3O-Ph-	$PhCH_2$-	903	62	2365	69	0.38	3.24
7g	Ph-	4-Cl-Ph-	CH_3-	1189	77	1985	83	0.60	4.22
7h	Ph-	4-Cl-Ph-	C_2H_5-	2285	60	ia	-	-	4.64
7i	Ph-	4-Cl-Ph-	C_4H_9-	ia	-	ia	-	-	5.58
7j	Ph-	4-Cl-Ph-	$PhCH_2$-	2130	53	6706	61	0.32	6.17
7k	Ph-	4-Br-Ph-	C_2H_5-	2237	45	5647	71	0.40	4.79
7l	Ph-	4-Br-Ph-	$PhCH_2$-	5025	78	712	69	7.06	6.24

ia = inactive at 10 μM

[a] E_{max} (%) is the percentage ratio between maximum fold induction of the tested compound and fold induction for **1** at 10 μM.

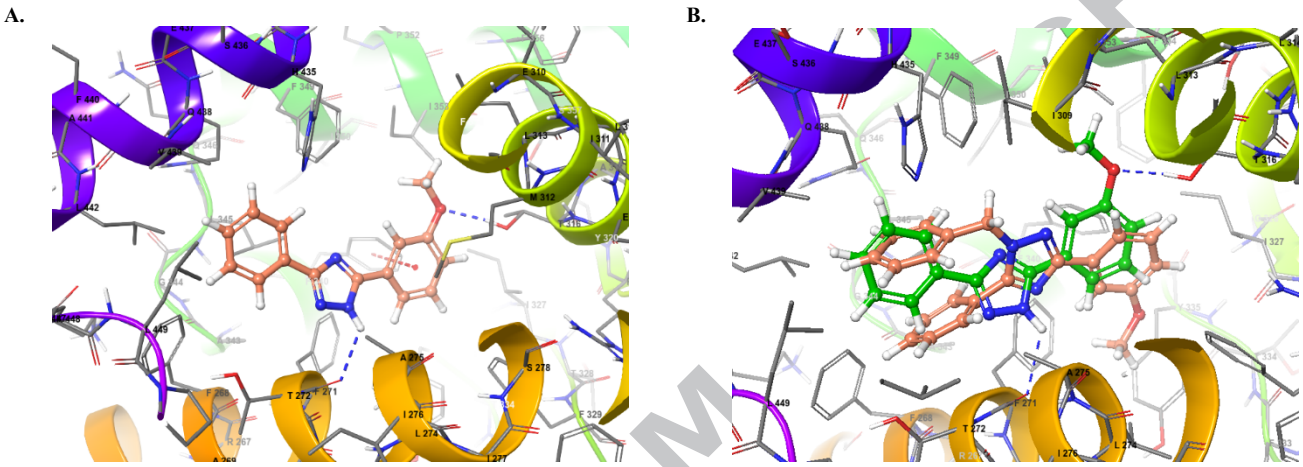

Figure 2. **A**. Molecular interactions of compound **6g** in the LBP of LXRβ. **B**. Overlay of compounds **6g** tautomer (green) and **7f** (pink). Hydrogen bonds are shown in blue dotted lines.

Alkylation of **6d** and **6e** with different alkyl groups afforded compound **7g-l**. These compounds showed similar pattern to their corresponding analogues **7a-f**, where they showed weak activity against both LXR isoforms. Compound **7l** showed good activity toward LXRβ (EC_{50} for LXRβ = 712 nM) and was 7-fold more selective to LXRβ over LXRα (Table 2). This compound was the most lipophilic among synthesized compounds (clogP = 6.24) and it was shown by Ishikawa that higher lipophilicity is important for LXRβ selectivity.[22] It is noteworthy that the ligand binding pockets for both LXRα and LXRβ are very similar. Therefore, rationalizing ligand selectivity to both receptors based on ligands' interactions only is not possible and other aspects of molecular recognition such as receptor-ligand dynamics and entropy should be taken into consideration.[11] Molecular dynamics simulations and free energy calculations are currently underway to determine the molecular basis of differential selectivity between LXRα and LXRβ.

We next explored the effect of acylating parent triazoles **6a**, **6e**, **6f**, **6g**, and **6i** using acetic anhydride to form acetyl derivatives **8a-e**. Substituting N-1 with acetyl group in **8a** lowered the agonistic activity toward LXRα by 2.8-fold, but increased the agonistic activity and selectivity toward LXRβ significantly (EC_{50} for LXRβ = 232 nM, EC_{50} α/β = 1.71) if compared to the parent triazole **6a**. Compound **8b** showed a higher agonistic activity toward LXRα and slight increase in E_{max} (58% for **8b** vs 55% for **6e**) if compared to **6e** (Table 1 and Table 3). The agonistic activity of **8b** toward LXRβ was significantly lower than **6e** but E_{max} increased from 62% to 78% (Table 1 and Table 3). Compound **8b** was 2-fold more selective for LXRα. Docking of compound **8b** in the LBP of LXRβ predicts that this compound is stabilized by forming a hydrogen bond with Thr316 and with van der Waals forces and hydrophobic contacts with surrounding residues such as Phe271, Ile327, Phe329, Leu313, Met312, Ile309, and Phe349 (Figure 3).

Acetylation of **6f** led to **8c**, which exhibited 3- and 4-fold lower activity against LXRα and LXRβ, respectively. Compound **8d** showed good agonistic activity against both LXR isoforms. There was no real difference in agonistic activity between **6g** and **8d** toward LXRα, while there was a change in EC_{50} from 68 nM in **6g** to 109 nM in **8d**. This difference was compensated slightly by increase in E_{max} from 72% in **6g** to 78% in **8d**. Compound **8e** showed more than 3- and 4-fold enhancement in agonistic activity over the parent **6i** toward LXRα and LXRβ, respectively. Similar to the parent **6i**, compound **8e** is 2-fold more selective toward LXRα over LXRβ.

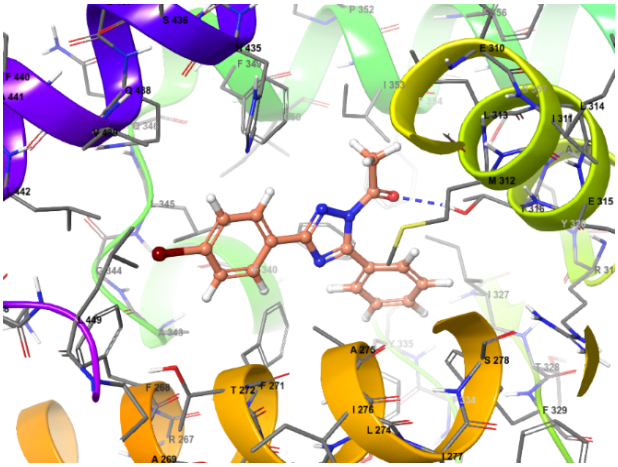

Figure 3. Molecular interactions of compound **8b** in the LBP of LXRβ. Hydrogen bonds are shown as blue dotted lines and π-π stacking interactions are shown as dotted red lines.

Finally, we explored the possibility of substituting N-1 with tosyl group by synthesizing **9a** and **9b**. Compound **9a** was > 4- and 12-fold less active against LXRα than the corresponding **6a** and **8a**, respectively. On the other hand, **9a** possess similar activity to **8a** against LXRβ and 3.9-fold higher activity than **6a** against the same isoform. Compound **9b** was completely inactive against both LXRα and LXRβ. We did not explore scaffold **9** further because it is not stable for long time at room temperature and tend to decompose to the parent triazole.

The SAR of synthesized compounds revealed that 3,5-disubstituted 1,2,4-triazoles are generally good modulators of LXR when the two substituents are phenyl rings or substituted phenyl rings (e.g. **6a-6g**). Substituting the phenyl ring at C-3 of the triazole ring with electron withdrawing groups make the compounds behave as dual agonists toward both LXR isoforms with slight selectivity toward LXRβ (e.g. **6b-6e**). Electron donating substituents at the same ring increased the potency toward both LXR isoforms significantly (e.g. **6f** and **6g**). Substituting C-3 of the triazole ring with pyridine renders the compound inactive (e.g. **6h**). Similarly, the compounds lost activity when C-5 was substituted with benzyl group (e.g. **6j-6l**). Substituting N-1 of the triazole ring with different alkyl groups led to mostly inactive compounds (e.g. **7a-7l**). On the other hand, substituting N-1 with acetyl group gave compounds of comparable potency to the parent triazole with higher efficacy (e.g. **8a-8d**).

We measured the effect of T0901317 (**1**), **6a-b**, and **8a-b** on gene expression of direct target genes of LXR: Fatty acid synthase (FAS), Sterol Regulatory Element Binding Protein 1c (SREBP-1c), 3-Hydroxy-3-Methylglutaryl-CoA Reductase (HMGCR), and LXRα. LXR agonists increase the expression of LXR target genes *FASN* and *SREBP-1c* in the liver causing increased *de novo* lipogenesis. Long term effects of increased expression of these genes can lead to hepatosteatosis, severe inflammation, and liver damage. We utilized the liver HepG2 immortalized cell line as a model to examine the effects of LXR ligands on these two genes. While we observed very efficacious agonist activity for T0901317 (**1**) in terms of induction of *FASN*, compounds **6a-b** and **8a-b** unexpectedly decreased FASN expression even though they behaved as agonists in both LXRα and LXRβ cotransfection assays. SREBP-1c is another gene that is involved in lipogenesis and T0901317 (**1**) increased expression of this gene almost 9-fold (Table 4). Compounds **6a-b** and **8a-b** that acted as agonists in the cotransfection assays and inverse agonists in terms of *FASN* expression had no effect on expression of the well characterized LXR target gene *SREBP-1c*. These data suggest that the 1,2,4-triazole compounds are a novel class of LXR modulators that display context dependent agonism/inverse agonism.

We calculated a set of physical descriptors and pharmaceutical properties of the selected compounds using Qikprop[23] to predict their absorption, distribution, metabolism, and excretion (ADME) properties (Table 5). All compounds comply with Lipniski's rule of five[24] and Jorgensen's rule of three[25] and are predicted to have good oral bioavailability and excellent absorption through cell membranes.

In conclusion, we have developed novel and potent LXR modulators based on 1,2,4-triazole scaffolds. Several of our new agonists exhibit good isoform selectivity in a cell based cotransfection assay where they generally behave as agonists. Interestingly, these compounds display "modulator" pharmacology since they function as inverse agonists in terms of FASN expression and are inactive on SREBP-1c expression in contrast to the activity observed in cotransfection assays. These new modulators possess excellent ADME properties and can be developed further to examine their unique modulator properties in vivo.

Acknowledgments

Bahaa Elgendy thanks the Science and Technology Development Fund (Egypt) for financial support (STDF-STF Grant 11969).

Table 3. LXR activity of 1,2,4-triazole derivatives **8a-e** and **9a-b**

				LXRα		LXRβ			
Comp.	**R¹**	**R²**	**R³**	**EC_{50} (nM)**	**E_{max} (%)**	**EC_{50} (nM)**	**E_{max} (%)**	**EC_{50} α/β**	**ClogP**
8a	Ph-	Ph-	CH_3CO-	396	56	232	63	1.71	2.84
8b	Ph-	4-Br-Ph-	CH_3CO-	113	58	231	78	0.49	3.43
8c	Ph-	4-CH_3-Ph-	CH_3CO-	228	53	351	62	0.65	3.15
8d	Ph-	3-CH_3O-Ph-	CH_3CO-	115	62	109	78	1.06	2.91
8e	Ph-	$PhCH_2$-	CH_3CO-	701	50	1425	68	0.49	3.20
9a	Ph-	Ph-	4-CH_3-C_6H_4-SO_2-	1705	75	259	81	6.58	3.66
9b	Ph-	3-CH_3O-Ph-	4-CH_3-C_6H_4-SO_2-	ia	-	ia	-	-	3.73

ia = inactive at 10 μM

[a] E_{max} (%) is the percentage ratio between maximum fold induction of the tested compound and fold induction for **1** at 10 μM.

Table 4. Normalized mRNA expression of *FASN* and *SREBP-1c* with **6a-b**, **8a-b**.

Gene	**Compound**	**Normalized mRNA Expression**	**SEM (+/-)**
FASN	T0901317 (**1**)	2.6210	0.630
	6a	0.7264	0.156
	6b	0.6393	0.390
	8a	0.6517	0.075
	8b	0.4448	0.091
SREBP-1c	T0901317 (**1**)	8.950	0.215
	6a	0.988	0.190
	6b	0.865	0.157
	8a	0.890	0.091
	8b	0.893	0.715

Table 5. Calculated Molecular Descriptors for Prediction of ADME properties for selected compounds. Recommended values or range for 95% of known drugs is shown in parenthesis.

Comp.	[a]mol_MW	[b]QPlogPo/w (-2 – 6)	[c]HBD (0 – 6)	[d]HBA	[e]% Human Oral Absorption	[f]PSA	[g]QplogS	[h]QPPCaco	[i]#metab (2 -8)	[j]QplogBB (-3 – 1.2)	[k]QPPMDCK

	(130 – 725)			(2-20)	(<25 % Low, > 80% High)	(7 – 200)	(-6.5 - .0.5)	(< 25 Poor, > 500 Excellent)			(< 25 Poor, > 500 Excellent)
6a	221.26	3.4	1	2.5	100	39.2	-4.012	2905.99	0	0.059	1567.17
6g	251.29	3.24	1	3.25	100	47.5	-4.27	2897.74	1	-0.016	1562.36
8a	263.298	2.84	0	5	100	53.2	-3.81	2973.15	0	0.042	1606.355
8b	342.194	3.428	0	5	100	53.1	-4.69	2973.84	0	0.216	4258.532
8d	293.324	2.9	0	5.7	100	61.1	-3.654	3028.45	1	-0.024	1638.673

[a]Molar weight in Daltons; [b]Logarithm of partitioning coefficient between *n*-octanol and water phases (range for 95% of drugs: -2 to 6); [c]Estimated number of hydrogen bonds that would be donated by the solute to water molecules in an aqueous solution. Values are averages taken over a number of configurations, so they can be non-integer.; [d] Estimated number of hydrogen bonds that would be accepted by the solute from water molecules in an aqueous solution.Values are averages taken over a number of configurations, so they can be non-integer; [e]Predicted human oral absorption on a 0 -100 % scale, based on a multiple linear regression model; [f]Polar surface area; [g]Predicted aqueous solubility, log S. S in mol dm^{-3}; [h]Predicted apparent Caco-2 cell permeability in nm/sec as a model for the gut-blood barrier. [i]Number of possible metabolic reactions; [j]Predicted brain/blood partition coefficient; [k]Predicted apparent MDCK cell permeability in nm/sec as a mimic for blood/ brain barrier. Qikrop predictions are for non-active transport.

References and notes

1. Jakobsson T, Treuter E, Gustafsson JÅ, Steffensen KR. *Trends Pharmacol Sci*. 2012;33(7):394-404.
2. El-Gendy B.-E. M, Goher S, Hegazy L, Arief MMH, Burris TP. Recent Advances in the Medicinal Chemistry of Liver X Receptors. *J Med Chem*. July 2018. doi:10.1021/acs.jmedchem.8b00045.
3. Zhu Y, Li Y. *ClinInvest Med*. 2009;32(5):E383-E394.
4. Katz A, Udata C, Ott E, et al. *J Clin Pharmacol*. 2009;49(6):643-649.
5. Wrobel J, Steffan R, Bowen SM, et al. *J Med Chem*. 2008;51(22):7161-7168.
6. Li N, Wang X, Liu P, et al. *Acta Pharm Sin B*. 2016;6(3):198-204. doi:10.1016/j.apsb.2016.03.005.
7. Viktorsson EÖ, Gabrielsen M, Kumarachandran N, et al. *Steroids*. 2017;118:119-127.
8. Hong C, Tontonoz P. *Nat Rev Drug Discov*. 2014;13(6):433-444.
9. A-González N, Castrillo A. *Biochim Biophys Acta - Mol Basis Dis*. 2011;1812(8):982-994.
10. Wang Y, Rogers PM, Stayrook KR, et al. *Mol Pharmacol*. 2008;74(6):1716-1721..
11. Stachel SJ, Zerbinatti C, Rudd MT, et al. *J Med Chem*. 2016;59(7):3489-3498..
12. Zhang R, Liu Z, Li Y, Wu B. *Int J Biochem Cell Biol*. 2016;78:180-185.
13. Pencheva N, Buss CG, Posada J, Merghoub T, Tavazoie SF. *Cell*. 2014;156(5):986-1001.
14. Flaveny CA, Griffett K, El-Gendy B.-E. M, et al. Cancer Cell. 2015:1-15.
15. García-Mediavilla MV, Pisonero-Vaquero S, Lima-Cabello E, et al. *Lab Investig*. 2012;92(8):1191-1202.
16. Griffett K, Solt LA, El-Gendy B.-E. M, Kamenecka TM, Burris TP. *ACS Chem Biol*. 2013;8(3):559-567.
17. Temml V, Voss C V., Dirsch VM, Schuster D. *J Chem Inf Model*. 2014;54(2):367-371.
18. Ghazvini Zadeh EH, El-Gendy B.-E. M, Pop AG, Katritzky AR. *MedChemComm*. 2012;3:52-55.
19. Maddila S, Pagadala R, Jonnalagadda S. *Lett Org Chem*. 2013;10(10):693-714.
20. Yeung KS, Farkas ME, Kadow JF, Meanwell NA. *Tetrahedron Lett*. 2005;46(19):3429-3432.
21. Katritzky AR, Wojciech K, Greenhill JV. *Recl des Trav Chim des Pays-Bas*. 1991;110(9):369-373.
22. Nomura S, Endo-Umeda K, Fujii S, Makishima M, Hashimoto Y, Ishikawa M. *Bioorg Med Chem Lett*. 2018;28(4):796-801.
23. Schrödinger Release 2018-3: QikProp, Schrödinger, LLC, New York, NY, 2018.
24. Lipinski CA, Lombardo F, Dominy BW, Feeney PJ. Experimental and computational approaches to estimate solubility and permeability in drug discovery and development settings1PII of original article: S0169-409X(96)00423-1. The article was originally published in Advanced Drug Delivery Reviews 23 (1997) 3. *Adv Drug Deliv Rev*. 2001;46(1):3-26. .
25. Jorgensen WL, Duffy EM. *Adv Drug Deliv Rev*. 2002;54(3):355-366.

Supplementary Material

Supplementary material that may be helpful in the review process should be prepared and provided as a separate electronic file. That file can then be transformed into PDF format and submitted along with the manuscript and graphic files to the appropriate editorial office.